Uniform warm dense matter formed by direct laser heating in the presence of external magnetic fields

D. Wu,[1,*] W. Yu,[2] Z. M. Sheng,[3,4] S. Fritzsche,[5,6] and X. T. He[7]

[1] *Institute for Fusion Theory and Simulation, Department of Physics, Zhejiang University, 310058 Hangzhou, China*
[2] *Shanghai Institute of Optics and Fine Mechanics, 201800 Shanghai, China*
[3] *USPA, Department of Physics, University of Strathclyde, Glasgow, G4 0NG, United Kingdom*
[4] *IFSA Collaborative Innovation Center, Shanghai Jiao Tong University, Shanghai, 200240, China*
[5] *Helmholtz Institut Jena, D-07743 Jena, Germany*
[6] *Theoretisch-Physikalisches Institut, Friedrich-Schiller-University Jena, D-07743 Jena, Germany*
[7] *Key Laboratory of HEDP of the Ministry of Education, CAPT, and State Key Laboratory of Nuclear Physics and Technology, Peking University, 100871 Beijing, China*

(Dated: November 18, 2019)

With the recent realization of kilotesla quasi-static magnetic fields, the interaction of laser with magnetized solids enters an unexplored new regime. In particular, a circularly polarized (CP) laser pulse may propagate in a highly magnetized plasma of any high density without encountering cut-off reflection in the whistler mode. With this, we propose a scheme for producing uniform warm dense matter (WDM) by direct laser heating with a CP laser irradiating onto the target along the magnetic field. It is shown by particle-in-cell simulations, which include advanced ionization dynamics and collision dynamics, moderately intense right-hand CP laser light at 10^{15}W/cm^2 can propagate in solid aluminium and heat it efficiently to 100 eV level within picosecond. By using two laser pulses irradiating from two sides of a thin solid target, uniform heating to WDM can be achieved. This provides a new controllable way to create WDM at different temperatures.

PACS numbers: 52.38.Kd, 41.75.Jv, 52.35.Mw, 52.59.-f

Introduction Warm dense matter (WDM) [1–3] is a particular matter associated with temperatures between 1 and 100 eV as well as densities between 0.1 and 10 times solid density. Until the present, however, little is known about the detailed behaviour of such WDM, since typically methods from both condensed-matter and high-temperature plasmas are needed in order to understand the behaviour of such matter in this regime. Experimentally, this state of matter is also difficult to reach since heating must occur on a time scale faster than the rapid expansion of the plasma. Until now, the majority of experimental data relevant to the WDM equation of state have come from strong shock experiments [4, 5]. While such measurements are crucial to guide the development of theoretical models, it enables one to access only a narrow range within temperature-density phase space.

Only recent progress helped produce WDM states far from the principal shock Hugoniot through the rapid, isochoric heating of a solid-density sample. This is achieved using heating drivers such as hot electrons [6] and MeV pulsed ions [7–10] produced by ultra (relativistic) intense and ultra short optical laser solid interactions, or direct irradiation of a sample by ultra bright x-rays from next-generation light sources [11–13]. For ultra (relativistic) intense and ultra short optical lasers, due to the complicated non-linear interaction with matter, the energy coupling mechanisms from lasers to electrons and ions are still now well understood, which makes it difficult to produce the WDM in a well controlled way. For irradiation of a sample by ultra bright x-rays, the absorption process in the sample is dominated by K-shell photo-absorption, ejecting a core electron into the continuum. After photoionization, the filling of the K-shell hole by Auger decay produces energetic electrons. Such energetic Auger electrons then heat the sample by collisions with other electrons and ions. The latter method is a significant breakthrough, especially due to the precise manipulation of energetic Auger electrons. However the temperature gradient of the produced WDM is very large [14]. Moreover access to such facilities is quite limited and any updated experimental set-up, such as shooting two opposite x-rays, is by no means impractical.

For a moderately intense laser, the majority of the incident is absorbed by electrons at front surface and within the skin depth of a target. Therefore, such interaction is insufficient for producing an uniform and large WDM sample. Recently, a peak field of 1200 Tesla [15], lasting microseconds, was generated by the electromagnetic flux-compression technique. Kilotesla magnetic fields can also be produced by a laser driven capacitor-coil target [16]. Moreover, production of self-generated tens-kilotesla magnetic fields was also reported through ultra high intensity laser interaction with matter [17–20]. The recent advances in high magnetic field production have opened a new realm of laser-plasma physics, which can be applied to generation of energetic particles and fast ignition of fusion targets [21–24]. Of particular interests is the propagation of a circularly polarized (CP) laser in the whistler regime in highly magnetized plasma. In such regime, laser can propagate in plasma of any density without encountering cut-off reflection. For the existing theory of whistler regime [25, 26], the laser plasma inter-

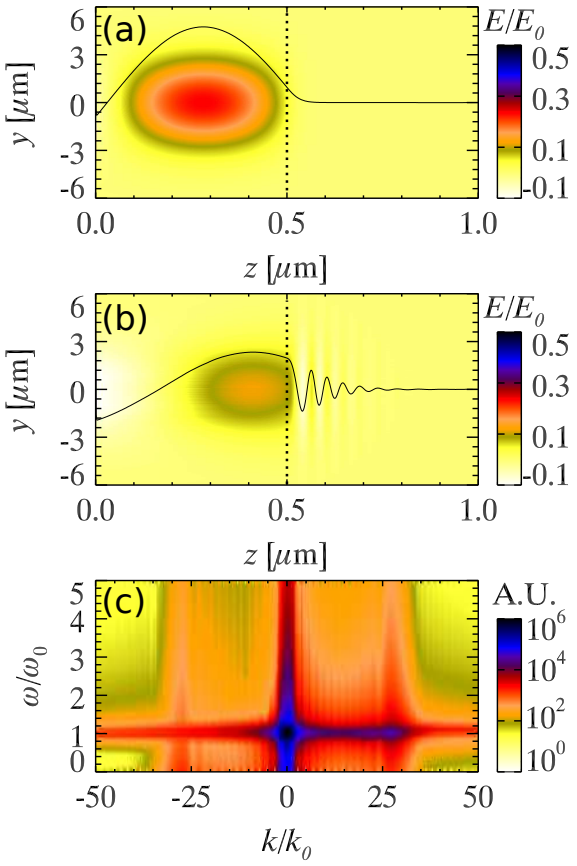

FIG. 1. (color online) The snapshot of electric fields E_x at $t = 10T_0$, where for (a) incident laser is of circularly polarized, and for (b) the laser is of circularly polarized with an external static magnetic field of $\tilde{B}_0 = 1.2$ along propagation direction. (c) frequency and wave number spectra of E_x along $y = 0$ for the whole simulation duration.

action is limited to the linear regime without considering collisional absorptions, and the plasma density and temperature are of constant.

In this Rapid Communication, we study the nonlinear laser plasma interaction in the whistler regime in dense plasma, taking into account the collision and ionization effects. Based upon this, we propose a novel scheme for the generation of uniform warm dense matter by direct laser heating. In order to avoid strong relativistic effects, we consider moderate laser intensity, $\sim 10^{15}$ W/cm^2. It is shown by particle-in-cell simulations, for realistic solid density plasmas, when both collisional absorption and ionization dynamics are of significant importance, a large fraction of the incident laser can still enter and propagate deep into the solid under the whistler regime. By combining two laser pulses, we propose a new controllable way to achieve the uniform heating of a solid sample.

Theory and simulations The propagation of the laser pulse within the plasma strongly depends on its polarization, intensity, the plasma density, absorptions, and the magnetic field strength and orientation, just to name a few. Here, let us briefly review the linear theory of CP light propagation along the embedded magnetic field $\boldsymbol{B}_0 = \tilde{B}_0\hat{\boldsymbol{z}}$ in a uniform over dense cold plasma [25], which is located in $z \geq 0$. The linear plasma dielectric constant can be written as $\epsilon_{B\mp} = 1 - \tilde{n}/(1 \mp \tilde{B}_0)$, where $\tilde{n} = \omega_p^2/\omega_0^2$ is the electron density normalized to the classical critical density $n_c = m\omega_0^2/4\pi e^2$, above which laser pulse can not propagate in unmagnetized plasma, here, $\tilde{B}_0 = \omega_c/\omega_0$ is the external magnetic field strength normalized to $m\omega_0 c/e$, e and m are the electron charge and mass, respectively, and ω_0 and ω_c are the laser and cyclotron frequencies, respectively. The minus and plus signs denote right and left-hand CP lasers, respectively. The laser electric field can be written as $\boldsymbol{E} = E\exp(i\omega_0 t + ik_z z)(\hat{\boldsymbol{x}} \pm i\hat{\boldsymbol{y}})$, where k_z and ω_0 are the wave vector and frequency, respectively, and which satisfy the linear dispersion relation $k_z^2 = \epsilon_{B\mp}$. Here, we have normalized $\tilde{k}_z$ with ω_0/c, and thus, we have $k_z^2 = 1$ in the vacuum ($z < 0$) and $k_z^2 = \epsilon_{B\mp}$ in the plasma. The solution of the laser equation for the normalized electric field $a = eE/m\omega_0 c$ is then $a = a_0 e^{iz} + a_R e^{-iz}$ for the incident and reflected light in the vacuum, and $a = a_T e^{ik_T z}$, where $k_T = \sqrt{\epsilon_{B\mp}}$, for the transmitted light in the plasma. In these notations, moreover, the subscripts 0, R, and T denote the incident, reflected (backward propagating), and transmitted quantities, respectively. The boundary condition that a and $\partial_z a$ be continuous at $z = 0$ leads to $a_R = a_0(k_T - 1)/(k_T + 1)$, so that the reflectivity is $\mathscr{R} = (a_R/a_0)^2 = (k_T - 1)^2/(k_T + 1)^2$, and therefore the transmissivity is $\mathscr{T} = 1 - \mathscr{R} = 4k_T/(k_T + 1)^2$. Note that from this linear theory above, we have $k_T > 1$ for $\tilde{B}_0 > 1$ and, hence, a considerable fraction of the incident right hand CP laser can propagate into over dense plasma.

In order to benchmark the linear theory as introduced above, two dimensional (2D) simulations by using the LAPINS [27–29] PIC code were carried out in the Z-Y Cartesian geometry. In these simulations, the size of the box is chosen to be Y (12 μm)×Z (1 μm), which is divided into 1200 × 1000 uniform grids. Here, a solid aluminium (with density 2.7 g/cm^3 and thickness 0.5 μm) is located at $z = 0.5$ μm. The initial temperature of aluminium solid is chosen to be 0.01 eV. The initial ionization degree of aluminium is $Z = 3$. The incident laser, intensity of 10^{15} W/cm^2, is normally focused on the target front with the pre-defined transverse profile $\exp(r^2/r_0^2)$, with $r_0 = 3\lambda_0$, and λ_0 is the central wavelength of the laser, i.e., 1 μm. Moreover, this pulse consists out of a $\sin^2$ rising front following with a constant-amplitude, where $T_0 = 3.3$ fs is the light-wave period. The external static magnetic field, with strength of $\tilde{B}_0 = 1.2$, is loaded along z direction. In the Z and Y directions, absorbing boundary conditions are applied for both particles and laser field. In Fig. 1, the snapshots of transverse electric field E_x are plotted at $t = 10T_0$, for (a) pure CP laser and (b) CP laser with an external static magnetic field of

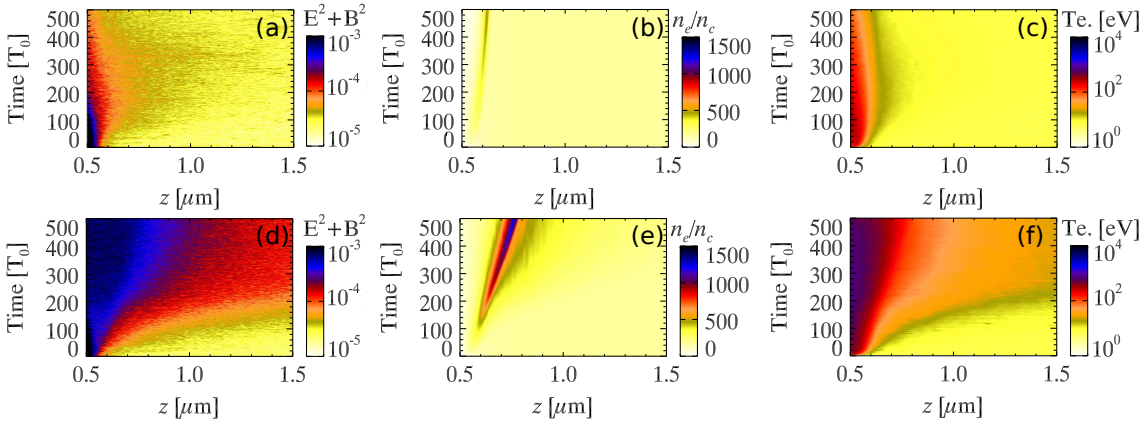

FIG. 2. (color online) Results for the electromagnetic field intensity, electron density and temperature as functions of time and position are shown for one dimensional simulations: the first row (a)-(c) for a CP laser without an external magnetic field, and the second row (d)-(f) for a CP laser with an external field of $\tilde{B}_0 = 1.2$. In these simulations, the ionization and collision dynamics are turned on.

$\tilde{B}_0 = 1.2$ along laser propagation direction, respectively. When compared with Fig. 1 (a) and (b), although the laser as shown in Fig. 1 (a) is completely reflected back, we can see a large fraction of laser electric field is transmitted into the solid in the whistler mode as shown in Fig. 1 (b). According to the linear plasma dielectric constant, i.e., $\epsilon_{B\mp} = 1 - \tilde{n}/(1 \mp \tilde{B}_0)$, the wavelength of the transmitted laser is $\sqrt{\epsilon_{B-}} \sim 30$ times smaller than the incident one, provided the frequency is kept the same. The predicted reduction of laser wavelength is well presented by the white curve on Fig. 1 (b). In Fig. 1(c), we also plotted frequency and wave number spectra of E_x along $y = 0$ for the whole simulation durations. Two peaks appear on this spectra plot, one located at $k = 0$ with $\omega = 1$, the other one located at $k = 30$ with $\omega = 1$. The first peak corresponds to the standing waves formed by incident and reflected lasers, and the second peak corresponds to the transmitted one. As expected, the 2D results are qualitatively consistent with the linear theory, indicating that parametric side-scattering instabilities that can appear in magnetized plasmas do not play a role in the space-time regime of interest here.

As we can see, in the whistler mode, a fraction of incident laser is transmitted into the plasmas. However, for the above linear regime, the collisional absorption process is not taken into account. For a realistic solid material, one also need to take into account ionization dynamics, this is because ionization will significant determine the plasma (free electron) density and therefore the absorption process. In addition, when temperature is lower than the Fermi energy, one has to take into account degenerate effects. Nowadays, such a comprehensive simulation is unavailable. Recently, the newly developed LAPINS code provides the possibility for such comprehensive however complicated simulations. This code incorporates both, the ionizaton [30] and collison dynamics [31] within the plasma on similar footings.

The ionization model contains both field ionization which usually dominated at the front of the target and impact ionizations which dominated at the inner target. In addition, for solid density plasmas, electron-ion recombination is not ignorable, and therefore in the LAPINS code, electron-ion recombination is also included in the ionization models. Among radiation recombination (RE), dielectronic recombination (DE) and three body recombination (TBR), TBR is the dominated one for solid density plasmas, as the cross section of TBR depend on n_e^2 while both RE and DE depend on n_e. For solid density plasmas, because of the strong shielding of surrounding charged particles, the ionization potential depression (IPD) effect appears. In the ionization model, the ionization potential used in the ionization model is therefore corrected by including this IPD effect. For a realistic solid target, it is usually partially ionized. The collision model contains both elastic collision and also inelastic collisions by taking into account ionization and excitation of bound electrons. In the LAPINS code, contributions from both the bound and free electrons are considered and organized in a self-consistent way, with electron-electron, electron-ion and ion-ion interactions modelled by means of the Monte-Carlo technique, similar to the one introduced by Takizuka [32] and Sentoku [33]. Such a collision technique is valid beyond the first-Born approximation, and thus is suitable for dealing with non-perturbative processes, e.g. coupled with self-generated or external static electromagnetic fields. Under low temperatures, the collision model also takes into account the degenerate effects. With this method, degenerate electrons are initialised according to the Fermi-Dirac distribution function, and scattering is via a Pauli blocked binary collision approximation. Such a Pauli blocking technique is widely used in the particle transport simu-

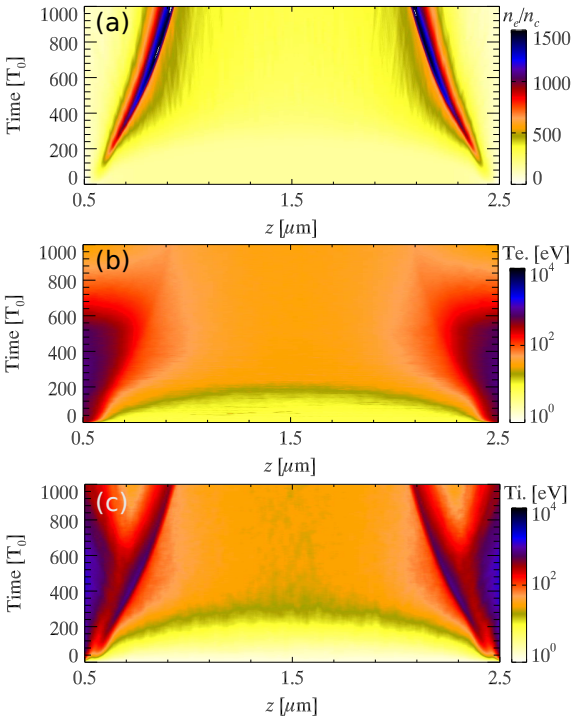

FIG. 3. (color online) Results for the electron density (a), electron temperature (b) and ion temperature (c) as functions of time and position are shown for CP lasers with an external magnetic field of $\tilde{B}_0 = 1.2$. In contrast to the results shown in Fig. 2, there are two CP incident lasers from the front and back sides. The laser pulses are turned off at $5 = 100T_0$. Other parameters are the same as shown in Fig. 2.

lations for semi-conductor devices [34]. These advanced features of the LAPINS code are critical for correctly studying laser solid interactions and high energy density laboratory astrophysics that lies in WDM regimes.

In order to avoid significant numerical noises, as the ionization could significantly increase the plasma (free electron) density, in the LAPINS code, we combine a fourth-order scheme of special difference with an implicit scheme of temporal stepping. This new scheme [27] can completely remove the numerical self-heating and significantly reduce the simulation burden when simulating solid density plasmas. Within the simulations, the ionization charge state and conductivity (or resistivity) of target could evolve according to the local plasma and electromagnetic fields conditions. Different types of materials can now be modelled based on their intrinsic atomic properties.

Taking the LAPINS code, with the newly developed ionization and collision dynamics models, laser solid interactions can be modelled close to real situation. When including collisions, such transmitted electromagnetic energy can efficiently convert to the plasmas, through inverse bremsstrahlung mechanism. When the plasma is significantly heated up, impact ionization then appears, which will update the plasma density and therefore the collision frequency. In Fig. 2, the electromagnetic field intensity, electron density and temperature, i.e. the average kinetic energy, of aluminium are presented as functions of time and positions by one dimensional simulations: the first row (a)-(c) for a CP laser without an external magnetic field, and the second row (d)-(f) for a CP laser with an external field of $\tilde{B}_0 = 1.2$. In Fig. 2, when compared (a)-(c) with (d)-(f), we find when the magnetic strength is larger than $\tilde{B}_0 \sim 1$, a large fraction of laser pulse is transmitted into the solid, and the solid bulk is dramatically heated and as expected, the free electron density due to ionization is also significantly increased. This threshold of magnetic strength, i.e. $\tilde{B}_0 > 1$, is consistent with the linear theory of CP laser propagation in whistler mode. Under such a regime, with the laser of intensity 10^{15} W/cm^2, the temperature of solid aluminium, as shown in Fig. 2 (f), can be as high as 100 eV, and the heated zone can be as large as micro-meters. We here produce a WDM state. Please note, when $\tilde{B}_0 < 1$, the solid is also moderately heated, and the heated depth is significantly larger than the skin depth. This is because, in the simulations, we have taken into account the electron-electron and electron-ion collisions, and therefore the effects of thermal conduction is included, which is responsible for the much larger heated zone beyond the skin depth.

Here please note, in Fig. 2 (e) and (f), the free electron density in the front of the target is significantly higher than the inner part. This is partially due to field ionization, as the laser intensity we used is already higher than field ionization threshold. In order to produce uniform WDM states, the above scheme as shown in Fig. 2 can be further optimized. As shown in Fig. 3, instead of taking only one CP laser pulse, we here take two CP laser pulses. Furthermore, instead of using semi-infinite laser pulse duration, here, the laser pulses are turned off at $t = 500T_0$. After the laser interaction, the system start to relax for another $500T_0$. Simulation indicate that an uniform WDM state of 100 eV spanned between 0.5 μm $< z <$ 2.5 μm is produced. Considering the expansion rate is determined ion acoustic speed, this WDM could last tens of picoseconds and proves to be very stable. By changing the external magnetic field strength, the transmissivity of CP laser can therefore be tuned, which could provide a controllable way for the production of WDM at different temperatures. In order to further increase the energy coupling efficiency based on this new scheme, two unidirectional transparent films can be placed in the front and back side of the target, such films allow unidirectional transmission of CP lasers. As the reflection does not change the polarization of CP lasers, the reflected CP lasers by such films can be regarded as new incident lasers but with lower intensities. This cycle will repeat itself until all laser contained energies are depleted.

Discussions and conclusions To summarize, a right-hand circularly polarized laser pulse can propagate in a sufficiently magnetized plasma of any density without encountering cut-off reflection in the whistler mode. With the recent realization of kilotesla magnetic fields, we here propose a novel scheme for the production uniform warm dense matter by direct laser heating in presence of external magnetic fields. It is shown by particle-in-cell simulations, which include advanced ionization dynamics and collision dynamics, moderately intense right-hand CP laser light at 10^{15}W/cm^2 can propagate in solid aluminium and heat it efficiently to the 100 eV level within picosecond. By using two laser pulses irradiating from two sides of a thin solid target, uniform heating to WDM can be achieved. By changing the external magnetic field strength, the transmissivity of CP laser can therefore be tuned, which could provide a controllable way for the production of WDM at different temperatures. This provides a new controllable way to create WDM at different temperatures. Such a uniform WDM would be of great importance for the measurements of equation of state and opacity in experiments. Our results also suggest that a CP laser might be useful for inertial confinement fusion together with a suitably magnetized fuel pellet.

This work was supported by Science Challenge Project (No. TZ2016005), National Natural Science Foundation of China (No. 11605269) and National Basic Research Program of China (Grant No. 2013CBA01504).

* Email: dwu.phys@zju.edu.cn

[1] T. G. White, N. J. Hartley, B. Borm, B. J. B. Crowley, J. W. O. Harris, D. C. Hochhaus, T. Kaempfer, K. Li, P. Neumayer, L. K. Pattison, F. Pfeifer, S. Richardson, A. P. L. Robinson, I. Uschmann, and G. Gregori, Phys. Rev. Lett. 112, 145005 (2014).
[2] A. Pelka, et al Phys. Rev. Lett. 105, 265701 (2010).
[3] G. M. Dyer, A. C. Bernstein, B. I. Cho, J. Osterholz, W. Grigsby, A. Dalton, R. Shepherd, Y. Ping, H. Chen, K. Widmann, and T. Ditmire, Phys. Rev. Lett. 101, 015002 (2008).
[4] V. E. Fortov, and I. V. Lomonosov, Shock Waves 20, 53 (2009).
[5] A. Benuzzi, T. Lower, M. Koenig, B. Faral, D. Batani, D. Beretta, C. Danson, and D. Pepler, Phys. Rev. E 54, 2162 (1996).
[6] I. Y. Skobelev, S. N. Ryazantsev, D. D. Arich, P. S. Bratchenko, A. Y. Faenov, T. A. Pikuz, P. Durey, L. Doehl, D. Farley, C. D. Baird, K. L. Lancaster, C. D. Murphy, N. Booth, C. Spindloe, P. McKenna, S. B. Hansen, J. Colgan, R. Kodama, N. Woolsey, S. A. Pikuz, Photonics Research, 6, 234 (2018).
[7] J. Kim, B. Qiao, C. McGuffey, M. S. Wei, P. E. Grabowski and F. N. Beg, Phys. Rev. Lett. 115, 054801 (2015).
[8] W. Bang, B. J. Albright, P. A. Bradley, E. L. Vold, J. C. Boettger, and J. C. Fernandez, Phys. Rev. E 92 063101 (2015).
[9] A. B. Zylstra, J. A. Frenje, P. E. Grabowski, C. K. Li, G. W. Collins, P. Fitzsimmons, S. Glenzer, F. Graziani, S. B. Hansen, S. X. Hu, M. Gatu Johnson, P. Keiter, H. Reynolds, J. R. Rygg, F. H. Seguin, and R. D. Petrasso, Phys. Rev. Lett. 114, 215002 (2015).
[10] S. Feldman, G. Dyer, D. Kuk, and T. Ditmire, Phys. Rev. E 95, 031201 (2017).
[11] S. M. Vinko, O. Ciricosta, B. I. Cho, K. Engelhorn, H. K. Chung, C. R. D. Brown, T. Burian, J. Chalupsky, et al Nature 482, 59 (2012).
[12] S. M. Vinko, et al Nat. Commun. 6, 6397 (2015).
[13] T. R. Preston, S. M. Vinko, O. Ciricosta, P. Hollebon, H. K. Chung, G. L. Dakovski, J. Krzywinski, M. Minitti, T. Burian, J. Chalupsky, V. Hajkova, L. Juha, V. Vozda, U. Zastrau, R. W. Lee, and J. S. Wark, Phys. Rev. Lett. 119, 085001 (2017).
[14] R. Royle, Y. Sentoku, R. C. Mancini, I. Paraschiv, and T. Johzaki, Phys. Rev. E 95, 063203 (2017).
[15] D. Nakamura, A. Ikeda, H. Sawabe, Y. H. Matsuda, and S. Takeyama, Review of Scientific Instruments 89, 095106 (2018).
[16] S. Fujioka, Z. Zhang, K. Ishihara, K. Shigemori, Y. Hironaka, T. Johzaki, A. Sunahara, N. Yamamoto, H. Nakashima, T. Watanabe, H. Shiraga, H. Nishimura, H. Azechi, Sci. Rep. 3, 1170 (2013).
[17] Z. M. Sheng and J. Meyer-ter-Vehn, Phys. Rev. E 54, 1833 (1996).
[18] J. P. Knauer, et al Phys. Plasmas 17, 056318 (2010).
[19] H. Yoneda, T. Namiki, A. Nishida, R. Kodama, Y. Sakawa, Y. Kuramitsu, T. Morita, K. Nishio, and T. Ide, Phys. Rev. Lett. 109, 125004 (2012).
[20] D. Wu, J. W. Wang, Plasma Phys. Control. Fusion 59, 095010 (2017).
[21] T. C. Wilson, F. Y. Li, M. Weikum, and Z. M. Sheng, Plasma Phys. Control. Fusion 59, 065002 (2017).
[22] D. Wu, S. X. Luan, J. W. Wang, W. Yu, J. X. Gong, L. H. Cao, C. Y. Zheng and X. T. He, Plasma Phys. Control. Fusion 59, 065004 (2017).
[23] A. Arefiev, T. Toncian and G. Fiksel, New J. Phys. 18, 105011 (2016).
[24] W. M. Wang, P. Gibbon, Z. M. Sheng and Y. T. Li, Phys. Rev. Lett. 114, 015001 (2015).
[25] F. F. Chen, Introduction to Plasma Physics and Controlled Fusion, 2nd ed. (Plenum, New York, 1984), Vol. 1.
[26] S. X. Luan, et al Phys. Rev. E 94, 053207 (2016).
[27] D. Wu, X. T. He, W. Yu, and S. Fritzsche, Phys. Rev. E 100, 013207 (2019).
[28] D. Wu, X. T. He, W. Yu, and S. Fritzsche, High Power Laser Science and Engineering 6, e50, (2018).
[29] H. Xu, W. W. Chang, H. B. Zhuo, L. H. Cao, and Z. W. Yue, Chin. J. Comput. Phys. 19, 305 (2002).
[30] D. Wu, X. T. He, W. Yu, and S. Fritzsche, Phys. Rev. E 95, 023208 (2017).
[31] D. Wu, X. T. He, W. Yu, and S. Fritzsche, Phys. Rev. E 95, 023207 (2017).
[32] T. Takizuka and H. Abe, J. Comput. Phys. 25, 205 (1977).
[33] Y. Sentoku and A. J. Kemp, J. Comput. Phys. 227, 6846 (2008)
[34] P. Lugli and D. K. Ferry, IEEE Transactions on Electron Devices, ED-32, 2431 (1985).